Two-color, nonlocal vector solitary waves with angular momentum in nematic liquid crystals

Two-color, nonlocal vector solitary waves with angular momentum in nematic liquid crystals

Gaetano Assanto,[1,*] Noel F. Smyth,[2,†] and Annette L. Worthy[3,‡]
[1]*NooEL—Nonlinear Optics and OptoElectronics Laboratory, Department of Electronic Engineering, INFN-CNISM, University "Roma Tre," Via della Vasca Navale 84, 00146 Rome, Italy*
[2]*School of Mathematics and Maxwell Institute for Mathematical Sciences, The King's Buildings, University of Edinburgh, Edinburgh EH9 3JZ, Scotland, United Kingdom*
[3]*School of Mathematics and Applied Statistics, University of Wollongong, Northfields Avenue, Wollongong, New South Wales 2522, Australia*
(Received 31 March 2008; published 22 July 2008)

The propagation and interaction of two solitary waves with angular momentum in bulk nematic liquid crystals, termed nematicons, have been studied in the nonlocal limit. These two spinning solitary waves are based on two different wavelengths of light and so are referred to as two-color nematicons. Under suitable boundary conditions, the two nematicons can form a bound state in which they spin about each other. This bound state is found to be stable to the emission of diffractive radiation as the nematicons evolve. In addition this bound state shows walk-off due to dispersion. Using an approximate method based on the use of suitable trial functions in an averaged Lagrangian of the two-color nematicon equations, modulation equations for the evolution of the individual nematicons are derived. These modulation equations are extended to include the diffractive radiation shed as the nematicons evolve. Excellent agreement is found between solutions of the modulation equations and full numerical solutions of the nematicon equations. The shed diffractive radiation is found to play a much lesser role in the nonlocal limit than in the local limit.

DOI: 10.1103/PhysRevA.78.013832 PACS number(s): 42.65.Tg, 42.70.Df

I. INTRODUCTION

The study of optical nonlinear guided waves in soft matter has seen a large increase of interest in recent years, examples of such soft media being nematic liquid crystals [1–4] and colloidal suspensions [5,6]. One reason for such interest is that such media have been shown to support stable, two dimensional solitary waves. In the context of nematic liquid crystals these solitary waves have been termed "nematicons" [3]. Soft media such as nematic liquid crystals, as well as being highly nonlinear, have the further important property of being nonlocal, in that the response of the medium to the light extends far beyond the waist of the light beam. This nonlocality is vital in that solitary wave solutions of (2+1)-dimensional nonlinear-Schrödinger- (NLS-) type equations are normally unstable, undergoing catastrophic collapse above an amplitude threshold [7]. Theoretical work by Conti *et al.* [2] showed that nematicons are stable due to their nonlocal interaction with the nematic. In addition the nematicon equations are the same as those governing a thermoelastic waveguide. Kuznetsov and Rubenchik [8] showed that solitary waves are stable in this additional context.

While the original work on nematicons considered the propagation of a single soliton [2–4,9–11], more recent work has considered the interaction of two nematicons of the same wavelength (color) [12] and two different wavelengths (colors) [13]. It was shown numerically [12] and experimentally [14] by Fratalocchi *et al.* for two interacting nematicons of the same color that if the two beams have angular momentum the attractive "force" due to the nematic can balance the repulsive centrifugal "force," so that a bound state can form with the two self-trapped beams rotating about each other. Moreover, the spin rate of the cluster can be controlled by acting on the input power [15]. This interaction of two nematicons of the same color, both in-phase and out-of-phase, was studied theoretically by García-Reimbert *et al.* [16] using the averaged Lagrangian-based modulation theory developed by Minzoni *et al.* [17] for the evolution of a single nematicon. This modulation theory had the advantage in that it can take account of the diffractive radiation shed by a nematicon as it evolves.

In previous work Skuse and Smyth [18] considered the interaction of two-color nematicons in the local limit by using the averaged Lagrangian method of García-Reimbert *et al.* [19,20]. In this limit catastrophic collapse is avoided due to the nematicon equations reducing to a pair of saturating NLS equations. Skuse and Smyth [18] were interested in the case in which the two colors formed a bound state, a vector nematicon. Due to the nonsymmetric optical parameters for the two colors, momentum conservation gives that the vector nematicon experiences walk-off. Here the term walk-off refers to a diffraction effect rather than optical anisotropy, the angular deviation of the Poynting vector from the wave vector. It is then the off-axis departure of each color (beam) component as it undergoes a different amount of diffraction while the system conserves linear and angular momentum. Excellent agreement was found for this walk-off as given by solutions of their modulation equations and by full numerical solutions. It was further found that the inclusion of the effect of the shed diffractive radiation was vital for this agreement. Without the inclusion of this radiation, the modulation walk-off differed from the numerical one by up to 30%, while when the radiation was included the difference was no more than 1%.

*assanto@uniroma3.it
†N.Smyth@ed.ac.uk
‡Annette_Worthy@uow.edu.au

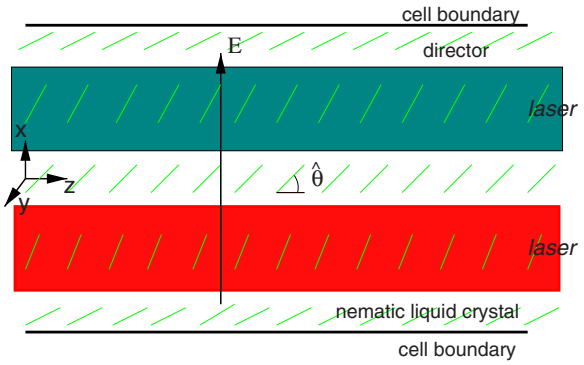

FIG. 1. (Color online) Schematic diagram of a liquid crystal cell with two polarized light beams of different colors.

In the present work the interaction of two different color nematicons with angular momentum will be studied in the highly nonlocal limit using the theoretical approach of Minzoni *et al.* [17] for a single nematicon. As for the local limit, the inclusion of the shed diffractive radiation will be found to be vital in order to obtain good agreement with full numerical solutions. However, the shed radiation is found to play much less of a role in the nematicon evolution than in the local limit case. Neglecting this radiation results in a decrease in agreement of around 5%, rather than the up to 30% decrease found in the local limit.

II. APPROXIMATE EQUATIONS

Let us consider two polarized, coherent light beams of two different wavelengths propagating through a cell filled with a nematic liquid crystal, as illustrated in Fig. 1. The light initially propagates in the z direction, with the (x,y) plane orthogonal to this. A static electric field is applied in the x direction so that in the absence of light the optical director is pre-tilted at an angle $\hat{\theta}$ to the z direction. Both input light beams are polarized with their electric fields in the x direction. Then let u and v be the electric field envelopes of the two light beams and θ be the perturbation of the optical director angle from its static value due to the light beams. In nondimensional form these equations are

$$i\frac{\partial u}{\partial z} + \frac{1}{2}D_u\nabla^2 u + A_u u \sin 2\theta = 0, \tag{1}$$

$$i\frac{\partial v}{\partial z} + \frac{1}{2}D_v\nabla^2 v + A_v v \sin 2\theta = 0, \tag{2}$$

$$\nu\nabla^2\theta - q \sin 2\theta = -2[A_u|u|^2 + A_v|v|^2]\cos 2\theta, \tag{3}$$

see Alberucci *et al.* [13]. The Laplacian ∇^2 is in the (x,y) plane. The coefficients D_u and D_v are the diffraction coefficients for the two colors and A_u and A_v are the coupling coefficients between the light and the nematic for the two colors. The parameter ν measures the elasticity of the nematic and q is related to the energy of the static electric field which pretilts the nematic [20].

The usual operating regime for nematicon propagation is the so-called nonlocal regime in which ν is large [2,4]. In this limit the reorientation of the nematic extends far past the optical beam(s), as measured by the waist(s) of the beam(s). Furthermore, in this limit, the deviation θ of the director from its equilibrium value is small, as can be seen from the director Eq. (3). So in the highly nonlocal limit the nematic Eqs. (1)–(3) can be approximated by

$$i\frac{\partial u}{\partial z} + \frac{1}{2}D_u\nabla^2 u + 2A_u u\theta = 0, \tag{4}$$

$$i\frac{\partial v}{\partial z} + \frac{1}{2}D_v\nabla^2 v + 2A_v v\theta = 0, \tag{5}$$

$$\nu\nabla^2\theta - 2q\theta = -2A_u|u|^2 - 2A_v|v|^2. \tag{6}$$

These nonlocal two-color nematicon equations have the Lagrangian

$$L = i(u^*u_z - uu_z^*) - D_u|\nabla u|^2 + 4A_u\theta|u|^2 + i(v^*v_z - vv_z^*) - D_v|\nabla v|^2 + 4A_v\theta|v|^2 - \nu|\nabla\theta|^2 - 2q\theta^2, \tag{7}$$

where the superscript asterisk denotes the complex conjugate.

As in Minzoni *et al.* [17] and Skuse and Smyth [18] an approximate solution of the highly nonlocal nematicon equations will be sought using appropriate trial functions in an averaged Lagrangian. Solutions will then be sought using self-similar trial functions of the form

$$u = a_u f(\chi_u/w_u)e^{i\psi_u} + ig_u e^{i\psi_u},$$

$$v = a_v f(\chi_v/w_v)e^{i\psi_v} + ig_v e^{i\psi_v},$$

$$\theta = \alpha_u(f(\chi_u/\beta_u))^2 + \alpha_v(f(\chi_v/\beta_v))^2, \tag{8}$$

where

$$\chi_u = \sqrt{(x-\xi_u)^2 + (y-\eta_u)^2},$$

$$\chi_v = \sqrt{(x-\xi_v)^2 + (y-\eta_v)^2},$$

$$\psi_u = \sigma_u + U_u(x-\xi_u) + V_u(y-\eta_u),$$

$$\psi_v = \sigma_v + U_v(x-\xi_v) + V_v(x-\eta_v). \tag{9}$$

The electric field amplitudes a_u, a_v, widths w_u, w_v, nematicon positions (ξ_u,η_u), (ξ_v,η_v), velocities (U_u,V_u), (U_v,V_v), phases σ_u, σ_v, shelf heights g_u, g_v and director pulse amplitudes α_u, α_v and widths β_u, β_v are functions of z. The first terms in the trial functions (8) for u and v are varying solitary waves, while the second terms represent the diffractive radiation of low wave number which accumulates under the evolving nematicons [17,21]. This shed radiation cannot remain flat, so it is assumed that $g_u(g_v)$ is nonzero in the disk $0 \le \sqrt{(x-\xi_u)^2+(y-\eta_u)^2} \le R_u$ $[0 \le \sqrt{(x-\xi_v)^2+(y-\eta_v)^2} \le R_v]$ [17,21]. In the case of the (1+1)-dimensional NLS equation the existence of this shelf of low wave number radiation under the pulse can be shown using inverse scattering [21].

The most widely used self-similar profiles f are a Gaussian [2] and a sech [17,18]. A sech profile is the same as that

for the soliton solution of the one-dimensional NLS equation. On the other hand, it was shown by Conti *et al.* [2] that the numerically determined two-dimensional nematicon solution has a Gaussian profile near its peak and its tail decays as the Bessel function K_0, due to circular symmetry. Hence a sech is a better approximation away from the peak of a nematicon, while a Gaussian is a better approximation around the peak. In this regard it was found by Skuse and Smyth [18] that in the limit of local interaction for ν small the particular choice of trial function made little difference to the final results. Hence both the sech and Gaussian profiles

$$f(r) = \text{sech } r \quad \text{and} \quad f(r) = e^{-r^2} \tag{10}$$

will be considered here.

The trial functions (8) are now substituted into the Lagrangian (7) for the nematicon equations and the averaged Lagrangian

$$\mathcal{L} = \int_{-\infty}^{\infty} \int_{-\infty}^{\infty} L dx dy \tag{11}$$

is calculated, from which the variational equations for the nematicon parameters are derived. For the Gaussian trial function all the required integrals can be evaluated. For the sech trial function all integrals, except cross integrals of the form

$$\int_{-\infty}^{\infty} \int_{-\infty}^{\infty} \theta |u|^2 dx dy, \tag{12}$$

can be evaluated. As in García-Reimbert *et al.* [19] and Minzoni *et al.* [17] approximate values for such integrals can be obtained using the idea of an "equivalent Gaussian," whereby in these integrals $\text{sech}^2(r/\beta)$ is replaced by the Gaussian $\exp[-r^2/(A\beta)^2]$and $\text{sech}^2(r/w)$ is replaced by the Gaussian $\exp[-r^2/(Bw)^2]$. The scaling parameters A and B are then calculated by matching the Taylor series of the integral (12) with the sech with the Taylor series with the "equivalent Gaussians" in the highly nonlocal limit $w_u/\beta_u \ll 1$. The details are as in Minzoni *et al.* [17], so that only the final results will be given here.

Substituting the trial functions (8) into the Lagrangian (7) then gives the averaged Lagrangian (11) as

$$\begin{aligned}
\mathcal{L} =& -2(I_2 a_u^2 w_u^2 + \Lambda_u g_u^2)(\sigma_u' - U_u \xi_u' - V_u \eta_u') - 2I_1 a_u w_u^2 g_u' \\
&+ 2I_1 g_u w_u^2 a_u' + 4I_1 a_u g_u w_u w_u' - 2(I_2 a_v^2 w_v^2 + \Lambda_v g_v^2)(\sigma_v' \\
&- U_v \xi_v' - V_v \eta_v') - 2I_1 a_v w_v^2 g_v' + 2I_1 g_v w_v^2 a_v' + 4I_1 a_v g_v w_v w_v' \\
&- D_u I_{22} a_u^2 - D_v I_{22} a_v^2 - D_u (I_2 a_u^2 w_u^2 + \Lambda_u g_u^2)(U_u^2 + V_u^2) \\
&- D_v (I_2 a_v^2 w_v^2 + \Lambda_v g_v^2)(U_v^2 + V_v^2) - 4\nu I_{42} \alpha_u^2 - 4\nu I_{42} \alpha_v^2 \\
&- 2qI_4 \alpha_u^2 \beta_u^2 - 2qI_4 \alpha_v^2 \beta_v^2 + \mathcal{L}_I.
\end{aligned} \tag{13}$$

The interaction component of the averaged Lagrangian is

$$\begin{aligned}
\mathcal{L}_I =& 2A_u A^2 B^2 a_u^2 w_u^2 [\alpha_u \beta_u^2 Q_1^{-1} + \alpha_v \beta_v^2 Q_2^{-1} e^{-\gamma_1}] \\
&+ 2A_v A^2 B^2 a_v^2 w_v^2 [\alpha_v \beta_v^2 Q_3^{-1} + \alpha_u \beta_u^2 Q_4^{-1} e^{-\gamma_2}] \\
&- 4\nu \alpha_u \alpha_v \beta_u^2 \beta_v^2 Q_5^{-2} [1 - \gamma_3] e^{-\gamma_3} - 2qA^2 \alpha_u \alpha_v \beta_u^2 \beta_v^2 Q_5^{-1} e^{-\gamma_3}.
\end{aligned} \tag{14}$$

Here

$$Q_1 = A^2 \beta_u^2 + B^2 w_u^2, \quad Q_2 = A^2 \beta_v^2 + B^2 w_u^2,$$

$$Q_3 = A^2 \beta_v^2 + B^2 w_v^2, \quad Q_4 = A^2 \beta_u^2 + B^2 w_v^2,$$

$$Q_5 = \beta_u^2 + \beta_v^2, \quad \gamma_1 = \frac{\rho^2}{Q_2}, \quad \gamma_2 = \frac{\rho^2}{Q_4}, \quad \gamma_3 = \frac{\rho^2}{A^2 Q_5},$$

$$\rho^2 = (\xi_u - \xi_v)^2 + (\eta_u - \eta_v)^2.$$

The integrals I_i, I_{ij} are

$$A = \frac{\sqrt{2} I_2}{\sqrt{I_{x32}}}, 1 \quad B = \sqrt{2 I_2}, 1, \quad I_1 = \int_0^{\infty} x f(x) dx = 2C, \frac{1}{2},$$

$$I_2 = \int_0^{\infty} x f^2(x) dx = \ln 2, \frac{1}{4},$$

$$I_{22} = \int_0^{\infty} x [f'(x)]^2 dx = \frac{1}{3} \ln 2 + \frac{1}{6}, \frac{1}{2}, \quad I_{x32} = \int_0^{\infty} x^3 f^2(x) dx$$

$$= 1.352301002 \cdots, \quad I_{42} = \frac{1}{4} \int_0^{\infty} x \left[\frac{d}{dx} f^2(x) \right]^2 dx = \frac{2}{15} \ln 2$$

$$+ \frac{1}{60}, \frac{1}{8}, \tag{16}$$

where C is the Catalan constant $C = 0.915965594 \cdots$ [22]. The first values of A, B and the integrals refer to the sech trial function, while the second values refer to the Gaussian trial function. There is no value given for I_{x32} for the Gaussian trial function as this integral is not needed. Finally

$$\Lambda_u = \frac{1}{2} R_u^2 \quad \text{and} \quad \Lambda_v = \frac{1}{2} R_v^2. \tag{17}$$

Taking variations of the averaged Lagrangian (13) results in the modulation equations

$$\frac{d}{dz} [I_2 a_u^2 w_u^2 + \Lambda_u g_u^2] = 0, \tag{18}$$

$$I_1 \frac{d}{dz} (a_u w_u^2) = \Lambda_u g_u \left[\sigma_u' - \frac{1}{2} D_u U_u^2 - \frac{1}{2} D_u V_u^2 \right], \tag{19}$$

$$\frac{d\xi_u}{dz} = D_u U_u, \quad \frac{d\eta_u}{dz} = D_u V_u, \tag{20}$$

$$\begin{aligned}
I_1 \frac{dg_u}{dz} =& \frac{1}{2} D_u I_{22} a_u w_u^{-2} - A_u A^2 B^4 a_u w_u^2 [\alpha_u \beta_u^2 Q_1^{-2} + \alpha_v \beta_v^2 Q_2^{-2} e^{-\gamma_1} \\
&- \alpha_v \beta_v^2 \rho^2 Q_2^{-3} e^{-\gamma_1}],
\end{aligned} \tag{21}$$

$$I_2\left[\frac{d\sigma_u}{dz}-\frac{1}{2}D_uU_u^2-\frac{1}{2}D_uV_u^2\right]$$
$$=-D_uI_{22}w_u^{-2}+A_uA^2B^2[\alpha_u\beta_u^2(A^2\beta_u^2+2B^2w_u^2)Q_1^{-2}$$
$$+\alpha_v\beta_v^2(A^2\beta_v^2+2B^2w_u^2)Q_2^{-2}e^{-\gamma_1}-\alpha_vw_u^2\beta_v^2\rho^2Q_2^{-3}e^{-\gamma_1}], \quad (22)$$

$$\frac{d}{dz}[(I_2a_u^2w_u^2+\Lambda_ug_u^2)U_u]$$
$$=-2A^2B^2(\xi_u-\xi_v)[A_u\alpha_va_u^2w_u^2\beta_v^2Q_2^{-2}e^{-\gamma_1}$$
$$+A_v\alpha_ua_v^2w_v^2\beta_u^2Q_4^{-2}e^{-\gamma_2}]+2q\alpha_u\alpha_v\beta_u^2\beta_v^2(\xi_u-\xi_v)Q_5^{-2}e^{-\gamma_3}$$
$$+4\nu A^{-2}\alpha_u\alpha_v\beta_u^2\beta_v^2(\xi_u-\xi_v)Q_5^{-3}[1-\rho^2Q_5^{-1}]e^{-\gamma_3} \quad (23)$$

$$\frac{d}{dz}[(I_2a_u^2w_u^2+\Lambda_ug_u^2)V_u]$$
$$=-2A^2B^2(\eta_u-\eta_v)[A_u\alpha_va_u^2w_u^2\beta_v^2Q_2^{-2}e^{-\gamma_1}$$
$$+A_v\alpha_ua_v^2w_v^2\beta_u^2Q_4^{-2}e^{-\gamma_2}]$$
$$+2q\alpha_u\alpha_v\beta_u^2\beta_v^2(\eta_u-\eta_v)Q_5^{-2}e^{-\gamma_3}$$
$$+4\nu A^{-2}\alpha_u\alpha_v\beta_u^2\beta_v^2(\eta_u-\eta_v)Q_5^{-3}[1-\rho^2Q_5^{-1}]e^{-\gamma_3} \quad (24)$$

plus the algebraic equations

$$2(2\nu I_{42}+qI_4\beta_u^2)\alpha_u$$
$$=A^2B^2\beta_u^2(A_ua_u^2w_u^2Q_1^{-1}+A_va_v^2w_v^2Q_4^{-1}e^{-\gamma_2})$$
$$-qA^2\alpha_v\beta_u^2\beta_v^2Q_5^{-1}e^{-\gamma_3}$$
$$-2\nu\alpha_v\beta_u^2\beta_v^2Q_5^{-2}(1-A^{-2}\rho^2Q_5^{-1})e^{-\gamma_3}, \quad (25)$$

$$qI_4\alpha_u=A^2B^4(A_ua_u^2w_u^4Q_1^{-2}+A_va_v^2w_v^4Q_4^{-2}e^{-\gamma_2})$$
$$+A_vA^4B^2a_v^2w_v^2\beta_u^2\rho^2Q_4^{-3}e^{-\gamma_3}-2\nu\alpha_v\beta_v^2Q_5^{-3}[\beta_v^2-\beta_u^2$$
$$-(\beta_v^2-3\beta_u^2)\rho^2A^{-2}Q_5^{-1}-A^{-4}\beta_u^2\rho^4Q_5^{-2}]e^{-\gamma_3}$$
$$-q\alpha_v\beta_v^2Q_5^{-2}(A^2\beta_v^2+\beta_u^2\rho^2Q_5^{-1})e^{-\gamma_3}, \quad (26)$$

for the nematicon parameters, together with symmetric equations for the v color. The modulation Eq. (18) is the equation for conservation of mass and modulation Eqs. (23) and (24) are the equations for conservation of the x and y momenta, respectively. These conserved quantities are in the sense of invariances of the Lagrangian (7) and do not all correspond to these quantities in the context of optics. For instance, Eq. (18) in the latter corresponds to conservation of power or photon number.

The final quantities to determine are the shelf radii R_u and R_v. In previous work on a single nematicon in the highly nonlocal limit [2,17] these radii were determined by linearizing the modulation equations about their fixed point, which resulted in a simple harmonic oscillator equation. The frequency of this oscillator was then matched to the nematicon frequency, which resulted in an expression for the shelf radius. While the same process could be performed for the two-color nematicon equations, the number of equations means that the resulting radii expressions are extremely complicated. In experiments the diffraction coefficients D_u and D_v and the coupling coefficients A_u and A_v take similar values. For instance, for the experiments of Alberucci *et al.* [13] the diffraction coefficients were 0.805 for red and 0.823 for near-infrared light. To calculate the shelf radii, it is then much simpler to take $D_u=D_v$ and $A_u=A_v$, in which case the radius expression of Minzoni *et al.* [17] can be used, suitably rescaled as this work had $D=1$ and $A=1$. These expressions are given in the Appendix.

Nöther's theorem applied to the Lagrangian (7) gives that the nematicons satisfy the energy conservation equation

$$\frac{dH}{dz}=\frac{d}{dz}\int_{-\infty}^{\infty}\int_{-\infty}^{\infty}[D_u|\nabla u|^2-4A_u\theta|u|^2+D_v|\nabla v|^2-4A_v\theta|v|^2$$
$$+\nu|\nabla\theta|^2+2q\theta^2]dxdy=0. \quad (27)$$

On substituting the trial functions (8) the final energy equation

$$\frac{dH}{dz}=\frac{d}{dz}[D_uI_{22}a_u^2+D_u(I_2a_u^2w_u^2+\Lambda_ug_u^2)(U_u^2+V_u^2)+D_vI_{22}a_v^2$$
$$+D_v(I_2a_v^2w_v^2+\Lambda_vg_v^2)(U_v^2+V_v^2)$$
$$-2A_uA^2B^2a_u^2w_u^2(\alpha_u\beta_u^2Q_1^{-1}+\alpha_v\beta_v^2Q_2^{-1}e^{-\gamma_1})$$
$$-2A_vA^2B^2a_v^2w_v^2(\alpha_v\beta_v^2Q_3^{-1}+\alpha_u\beta_u^2Q_4^{-1}e^{-\gamma_2})$$
$$+4\nu I_{42}(\alpha_u^2+\alpha_v^2)+2qI_4(\alpha_u^2\beta_u^2+\alpha_v^2\beta_v^2)$$
$$+4\nu\alpha_u\alpha_v\beta_u^2\beta_v^2Q_5^{-2}(1-A^{-2}\rho^2Q_5^{-1})e^{-\gamma_3}$$
$$+2qA^2\alpha_u\alpha_v\beta_u^2\beta_v^2Q_5^{-1}e^{-\gamma_3}]=0 \quad (28)$$

results. On making the symmetry assumption discussed above, the fixed point of the modulation equations can then be found from this energy equation and the relations determined by looking for the steady states of Eqs. (19) and (21) and their v color equivalents. This fixed point will be required below, particularly in the calculation of radiation loss.

Adding the momentum Eqs. (23) and (24) to their v color counterparts gives the equations for total momentum conservation in the x and y directions as

$$\frac{d}{dz}[(I_2a_u^2w_u^2+\Lambda_ug_u^2)U_u+(I_2a_v^2w_v^2+\Lambda_vg_v^2)U_v]=0 \quad (29)$$

and

$$\frac{d}{dz}[(I_2a_u^2w_u^2+\Lambda_ug_u^2)V_u+(I_2a_v^2w_v^2+\Lambda_vg_v^2)V_v]=0, \quad (30)$$

respectively. Let us consider boundary conditions for which the two nematicons form a bound state and denote these boundary values by a subscript 0. Let us further assume that the nematicons evolve to have the same position as $z\to\infty$ and denote final steady state values by a hat superscript. Then on noting mass conservation (18) and total momentum conservation in the x and y directions and that $g_{u0}=g_{v0}=0$ and $\hat{g}_u=\hat{g}_v=0$, we have that the walk-off of the bound state nematicon is given by

$$\hat{\xi}' = \hat{\xi}'_u = \hat{\xi}'_v = \frac{D_u D_v P_{x0}}{I_2(D_v a_{u0}^2 w_{u0}^2 + D_u a_{v0}^2 w_{v0}^2)} \tag{31}$$

and

$$\hat{\eta}' = \hat{\eta}'_u = \hat{\eta}'_v = \frac{D_u D_v P_{y0}}{I_2(D_v a_{u0}^2 w_{u0}^2 + D_u a_{v0}^2 w_{v0}^2)}, \tag{32}$$

where

$$P_{x0} = I_2 a_{u0}^2 w_{u0}^2 U_{u0} + I_2 a_{v0}^2 w_{v0}^2 U_{v0} \tag{33}$$

and

$$P_{y0} = I_2 a_{u0}^2 w_{u0}^2 V_{u0} + I_2 a_{v0}^2 w_{v0}^2 V_{v0} \tag{34}$$

are the initial x and y momenta. Combining the two momentum conservation expressions (31) and (32) gives the radial walk-off of the vector nematicon as

$$\rho'_w = \sqrt{\hat{\xi}'^2 + \hat{\eta}'^2}. \tag{35}$$

III. KEPLER COORDINATES

The modulation Eqs. (18)–(26) for the u color and their symmetric v counterparts consist of two basically independent oscillations, one oscillation being an amplitude and width oscillation in $a_{u(v)}$, $w_{u(v)}$ and $g_{u(v)}$, and the other a position and velocity oscillation in $\xi_{u(v)}$, $\eta_{u(v)}$, $U_{u(v)}$, and $V_{u(v)}$. The position and velocity oscillation possesses a close connection with the two body gravitational problem. This can be more clearly seen by transforming the position and velocity Eqs. (20), (23), and (24) and their symmetric v equivalents to polar coordinates centered on the "center of mass" of the two-color nematicons. This has the added advantage of making the position and velocity equations much cleaner.

We define the "masses" M_u of the u color and M_v of the v color as

$$M_u = I_2 a_u^2 w_u^2 + \Lambda_u g_u^2 \quad \text{and} \quad M_v = I_2 a_v^2 w_v^2 + \Lambda_v g_v^2. \tag{36}$$

The positions of the two nematicons can be written in vector form as $\vec{\xi}_u = (\xi_u, \eta_u)$ for the u color and $\vec{\xi}_v = (\xi_v, \eta_v)$ for the v color. The polar coordinate system is then based on the "center of mass" of the two-color nematicons

$$\vec{R} = \frac{D_v M_u \vec{\xi}_u + D_u M_v \vec{\xi}_v}{D_v M_u + D_u M_v}, \tag{37}$$

with the relative displacement of the nematicons

$$\vec{\rho} = \vec{\xi}_u - \vec{\xi}_v. \tag{38}$$

In this center-of-mass system, the distance from the center-of-mass is ρ and the polar angle is ϕ. The equations for the position of the two-color nematicons are then the conservation of angular momentum equation

$$\rho^2 \frac{d\phi}{dz} = L, \tag{39}$$

where L is a constant and the radial equations

$$\frac{d\vec{R}}{dz} = \vec{0} \tag{40}$$

and

$$\frac{d^2\rho}{dz^2} - L^2 \rho^{-3} = -\frac{D_v M_u + D_u M_v}{M_u M_v} \frac{\partial \Phi}{\partial \rho}. \tag{41}$$

The potential Φ is

$$\begin{aligned} \Phi = & -2A_u A^2 B^2 \alpha_v a_u^2 w_u^2 \beta_v^2 Q_2^{-1} e^{-\gamma_1} \\ & - 2A_v A^2 B^2 \alpha_u a_v^2 w_v^2 \beta_u^2 Q_4^{-1} e^{-\gamma_2} \\ & + 4\nu \alpha_u \alpha_v \beta_u^2 \beta_v^2 Q_5^{-2} (1 - A^{-2} \rho^2 Q_5^{-1}) e^{-\gamma_3} \\ & + 2qA^2 \alpha_u \alpha_v \beta_u^2 \beta_v^2 Q_5^{-1} e^{-\gamma_3}. \end{aligned} \tag{42}$$

The potential (42) is attractive and the Hamiltonian has a minimum, so that there exists a stable orbit for the two-color nematicons. The position evolution of the two-color nematicons then has an exact analogy with the classical two body problem from Newtonian gravitation. However, for the two-color nematicon interaction the potential is Gaussian, with a rather involved form, rather than the inverse ρ potential of gravitation.

IV. DIFFRACTIVE RADIATION LOSS

The modulation equations of the previous two sections are not complete yet as the effect of the diffractive radiation shed by the nematicons as they evolve has not yet been included. As the amplitude of the shed radiation is much less than the amplitude of the nematicons, this radiation is governed by the linearized electric field equations

$$\begin{aligned} i\frac{\partial u}{\partial z} + \frac{1}{2r} D_u \frac{\partial}{\partial r}\left(r \frac{\partial u}{\partial r}\right) = 0, \\ i\frac{\partial v}{\partial z} + \frac{1}{2r} D_v \frac{\partial}{\partial r}\left(r \frac{\partial v}{\partial r}\right) = 0, \end{aligned} \tag{43}$$

which are just the Schrödinger equation. This radiation problem has already been studied by García-Reimbert *et al.* [17], so that the details will not be repeated here. The final result is that the mass conservation Eq. (18) and Eq. (21) for g_u are replaced by

$$\frac{d}{dz}(I_2 a_u^2 w_u^2 + \Lambda_u g_u^2) = -2D_u \delta_u \tilde{\Lambda}_u \kappa_u^2 \tag{44}$$

and

$$\begin{aligned} I_1 \frac{dg_u}{dz} = & \frac{1}{2} D_u I_{22} a_u w_u^{-2} - A_u A^2 B^4 a_u w_u^2 [\alpha_u \beta_u^2 Q_1^{-2} + \alpha_v \beta_v^2 Q_2^{-2} e^{-\gamma_1} \\ & - \alpha_v \beta_v^2 \rho^2 Q_2^{-3} e^{-\gamma_1}] - 2D_u \delta_u g_u, \end{aligned} \tag{45}$$

respectively, where the loss coefficient δ_u is

$$\delta_u = -\frac{\sqrt{2\pi}I_1}{2e\kappa_u\tilde{\Lambda}_u}\int_0^z \pi\kappa_u(z')\ln[(z-z')/\tilde{\Lambda}_u] \times\left\{\left[\left(\frac{1}{2}\ln[(z-z')/\tilde{\Lambda}_u]\right)^2+\frac{3\pi^2}{4}\right]^2 + \pi^2\{\ln[(z-z')/\tilde{\Lambda}_u]\}^2\right\}^{-1}\frac{dz'}{(z-z')} \quad (46)$$

and

$$\kappa_u^2 = \frac{1}{\tilde{\Lambda}_u}[I_2 a_u^2 w_u^2 - I_2\hat{a}_u^2\hat{w}_u^2 + \tilde{\Lambda}_u g_u^2]. \quad (47)$$

The variable κ_u measures the difference between the mass of the u color at z and its mass at the fixed point. The mass equation for the v color and the equation for g_v are obtained by the obvious symmetric substitutions. Finally

$$\tilde{\Lambda}_u = \frac{1}{2}(7\beta_{u1/2})^2, \quad \beta_{u1/2} = \beta_u \operatorname{sech}^{-1}(1/\sqrt{2}). \quad (48)$$

V. RESULTS

In this section solutions of the modulation Eqs. (19), (20), (22)–(26), (44), and (45) and their symmetric v color counterparts will be compared with full numerical solutions of the two-color nematicon Eqs. (1)–(3). The modulation equations were solved using the standard fourth order Runge-Kutta method. The full nematicon Eqs. (1)–(3) were solved using the method described in Skuse and Smyth [18], so this method will not be described again here.

In deriving the modulation equations it was assumed that the director angle θ was small, so that $\sin 2\theta$ and $\cos 2\theta$ could be approximated by the first terms in their Taylor series. It was found from numerical solutions that for this approximation to be valid, the nonlocality parameter ν was required to be $O(100)$, in which case $\theta \sim 0.1$. In contrast, in Minzoni *et al.* [17] for a single nematicon the small θ approximation was valid for $\nu \sim 10$, while for two-color nematicons $\theta \sim 0.3-0.4$ for $\nu=10$. The difference for two interacting nematicons is that the nematicons are in fairly close proximity and overlap to some extent, so that as the director is forced by the sum of the powers of the two colors, as can be seen from the director Eq. (3), the forcing is increased over a single nematicon. Now as ν increases, θ decreases. Furthermore as ν increases, the further apart the two colors can be and still form a bound state due to nonlocality. So for the examples of this section, the value $\nu=500$ was chosen, which is at the upper end of the usual experimental range from $O(10)-O(100)$ [2].

Let us first consider comparisons for the sech initial condition. Figure 2 shows the walk-off comparison for the initial values and parameters indicated. In this figure

$$\rho_u = [\xi_u^2 + \eta_u^2]^{1/2} \quad \text{and} \quad \rho_v = [\xi_v^2 + \eta_v^2]^{1/2}, \quad (49)$$

so that ρ_u and ρ_v measure the distances of the nematicons from the axis, which is a measure of their walk-off [11]. It can be seen that there is good agreement for the walk-off as

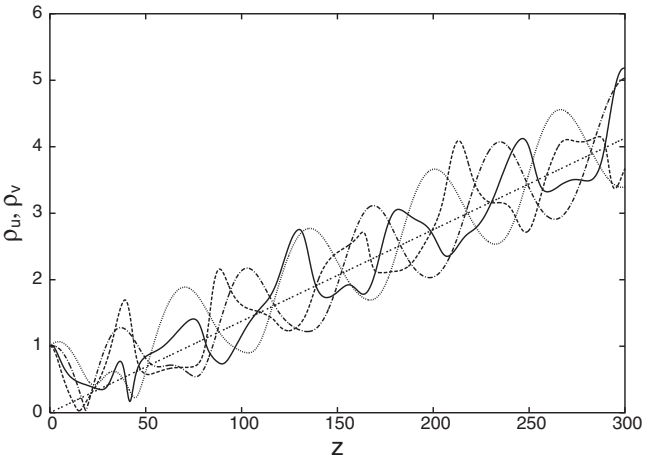

FIG. 2. Radial positions of nematicons for the initial values $a_u=1.8$, $a_v=1.8$, $w_u=3.0$, $w_v=3.0$, $\xi_u=1.0$, $\xi_v=-1.0$, $\eta_u=\eta_v=0.0$, $U_u=0.03$, $U_v=-0.01$, $V_u=0.03$, $V_v=-0.01$ with $\nu=500$, $q=2$, $A_u=1.0$, $A_v=0.95$, $D_u=1.0$, $D_v=0.98$. Full numerical solution, u color (—); v color (— — —); solution of modulation equations for u color (· · ·); v color (— · — · —); momentum conservation result (35) (· · · .. · · ·).

given by the full numerical and modulation solutions, particularly up to $z=100$. After this point, there is some period difference between the solutions. Furthermore the modulation solution settles to a more harmonic oscillation faster than the numerical solution. Also shown in this figure is the walk-off of the bound state given by Eq. (35). This line shows that the walk-off of the orbiting nematicons is given nearly exactly by momentum conservation, so that there is little momentum being shed in diffractive radiation, in agreement with experimental reports [15]. This is in contrast to the local limit for which momentum loss to radiation is significant [18]. In Skuse and Smyth [18] a comparison was made between the walk-off angle as given by the full numerical and modulation solutions. In this local limit the nematicons did not have angular momentum and their trajectories rapidly settled to a straight line, making such a comparison possible. However in the present nonlocal limit the nematicons remain in an orbit about each other and do not settle to a straight walk-off. Furthermore the numerical walk-off path is not harmonic, even after $z=400$. Therefore it is not possible to make a similar comparison here.

The comparison of Fig. 2 was for small angular velocities. Figure 3 shows comparisons for much larger angular velocities. The walk-off comparison shown in Fig. 3(a) shows similar good agreement between the numerical and modulations solutions, again particularly up to $z=100$, with some period difference for larger z. However for this example, there is about a 5% difference between the momentum conservation trajectory (35) and the mean of the modulation trajectories, showing that radiation loss is of some importance for higher angular velocities. The main difference between the results for small and relatively larger angular velocities is shown in Fig. 3(b), where an amplitude comparison is shown. It can be seen that while there is agreement in the means of the amplitude oscillation, the numerical amplitude oscillation picks up a second frequency. This sec-

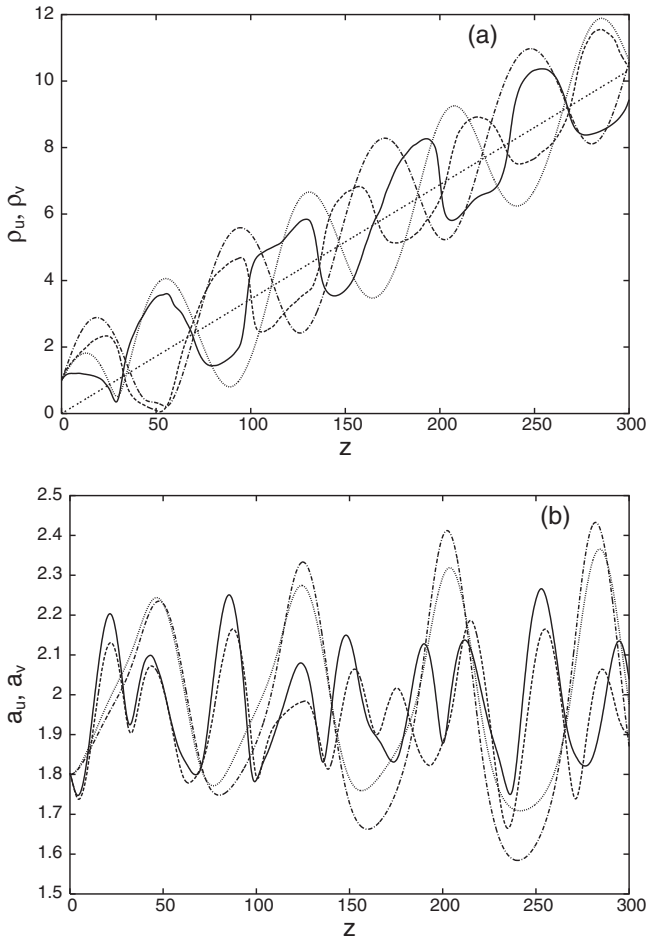

FIG. 3. Comparisons for the initial values $a_u=1.8$, $a_v=1.8$, $w_u=3.0$, $w_v=3.0$, $\xi_u=1.0$, $\xi_v=-1.0$, $\eta_u=\eta_v=0.0$, $U_u=0.1$, $U_v=-0.15$, $V_u=0.1$, $V_v=-0.15$ with $\nu=500$, $q=2$, $A_u=1.0$, $A_v=0.95$, $D_u=1.0$, $D_v=0.98$. Full numerical solution, u color (—); v color (— — —); solution of modulation equations for u color (· · ·); v color (— · — · —); (a) Radial postions, momentum conservation result (35) (· · · ·· · · ·); (b) amplitudes.

ond frequency was also noted by García-Reimbert *et al.* [16] for the case of two interacting nematicons of one color. It is due to the nematicons becoming elliptical in cross-section due to the "high" angular velocity, the second frequency being the oscillation in the major and minor axes of the ellipse. For the example shown in Fig. 3 the ratio of the minor to major axis is about 0.7. For low angular velocities, the nematicons remain circular and the second frequency is not seen. As noted in García-Reimbert *et al.* [16] extending the trial functions (8) to have an elliptical cross-section is not worth the effort as it would make extended modulation equations ever more extended, even if all the integrals could be computed.

Similar comparisons could be made for the Gaussian trial function. However, it was found that for the Gaussian trial function, the small θ approximation became valid only for $\nu=2000$ and higher, which is above the usual experimental range. This is in contrast to the local limit, in which case the comparison between the modulation and full numerical solutions was found to be nearly independent of the choice of trial function [18]. For $\nu=2000$ and higher, the comparison between the modulation and numerical solutions for the Gaussian trial function is similar to that for the sech trial function, so no results will be reported here.

VI. CONCLUSIONS

The interaction of two nematicons of different wavelengths (colors) has been considered in the highly nonlocal limit. This interaction was analyzed using suitable trial functions in an averaged Lagrangian formulation, resulting in modulation equations for the nematicon parameters. These modulation equations were shown to have a close connection to the equations for the two body gravitational problem, but with a potential that was Gaussian (and attractive). Therefore a vector nematicon solution consisting of the two nematicons orbiting about each other exists, which was found to be stable with respect to shed diffractive radiation. This is in contrast to the opposite local limit, in which the diffractive radiation was found to have a dominant role [18]. This decreasing effect of radiation as nonlocality increases is in agreement with the work of Minzoni *et al.* [17] for the evolution of single nematicons. The close connection between the equations governing multicolored nematicons and gravitation should allow further multicolored nematicon interactions to be investigated. This is the subject of current investigations.

ACKNOWLEDGMENT

This research was supported by the Engineering and Physical Sciences Research Council (EPSRC) under Grant No. EP/C548612/1.

APPENDIX: SHELF RADIUS

The shelf radii R_u and R_v are determined by linearizing the modulation Eqs. (18)–(26) and their symmetric v counterparts about their fixed point. After some algebra this results in the simple harmonic oscillator equation

$$\frac{d^2 g_u}{dz^2} - \frac{\Theta \Lambda_u \hat{\Sigma}_u'}{I_1^2(\hat{w}_u^2 + 2\hat{a}_u \hat{w}_u \varphi)} g_u = 0 \tag{A1}$$

and a similar equation for g_v, where

$$\hat{\Sigma}_u' = \hat{\sigma}_u' - \frac{1}{2} D_u \hat{U}_u^2 - \frac{1}{2} D_u \hat{V}_u^2, \tag{A2}$$

$$\varphi = \frac{D_u I_{22} \Gamma^2 - A_u A^2 B^2 \hat{w}_u^2 \hat{\beta}_u^2 \Gamma (2\hat{\alpha}_u + \hat{a}_u W_1)}{A_u A^2 B^2 \hat{a}_u \hat{w}_u \hat{\beta}_u \Phi}, \tag{A3}$$

$$\Phi = 2A^2 \hat{\alpha}_u \hat{\beta}_u^3 + \hat{w}_u \hat{\beta}_u W_2 \Gamma + 2B^2 \hat{w}_u^3 \hat{\alpha}_u W_0, \tag{A4}$$

$$W_0 = \frac{2q(I_4 + A^2/4) B^2 \hat{w}_u \hat{\beta}_u^2 + \nu(8I_{42} + 1) B^2 \hat{w}_u}{2q\hat{\beta}_u (I_4 + A^2/4)(2A^2 \hat{\beta}_u^2 - B^2 \hat{w}_u^2)}, \tag{A5}$$

$$W_1 = \frac{4A_u A^2 B^4 \hat{a}_u \hat{w}_u^4}{q(I_4 + A^2/4)\Gamma^2}, \quad \Gamma = A^2\hat{\beta}_u^2 + B^2\hat{w}_u^2, \tag{A6}$$

$$W_2 = \frac{8A_u A^4 B^4 \hat{a}_u^2 \hat{w}_u^3 \hat{\beta}_u}{q(I_4 + A^2/4)\Gamma^3}(\hat{\beta}_u - \hat{w}_u W_0), \tag{A7}$$

$$\Theta = \frac{D_u I_{22}}{2\hat{w}_u^2}\left[Q_0 - \frac{Q_1 + Q_2}{\hat{\alpha}_u \hat{w}_u \hat{\beta}_u}\right], \quad Q_0 = 1 - \frac{2\hat{a}_u \varphi}{\hat{w}_u}, \tag{A8}$$

$$Q_1 = \hat{w}_u \hat{\beta}_u [\hat{\alpha}_u + \hat{a}_u (W_1 + \varphi W_2)], \tag{A9}$$

$$Q_2 = 2\hat{\alpha}_u \hat{a}_u \varphi (A^2 \hat{\beta}_u^2 - B^2 \hat{w}_u^2)(\hat{\beta}_u - W_0)\Gamma^{-1}. \tag{A10}$$

As in Kath and Smyth [21] and Minzoni *et al.* [17], the frequency of the simple harmonic oscillator (A1) is then matched to the nematicon oscillation frequency $\hat{\Sigma}_u'$, given by Eq. (22) as

$$\hat{\Sigma}_u' = 2A_u A^2 B^2 \hat{\alpha}_u \hat{w}_u^2 \hat{\beta}_u^2 (A^2 \hat{\beta}_u^2 - 2B^2 \hat{w}_u^2)(I_2 \Gamma^2)^{-1}. \tag{A11}$$

This results in

$$\Lambda_u = -\frac{\hat{\Sigma}_u' I_1^2 \hat{w}_u (\hat{w}_u + 2\hat{a}_u \varphi)}{\Theta}. \tag{A12}$$

The shelf radius R_v and Λ_v for the v color is found by symmetry.

[1] M. Peccianti, G. Assanto, A. de Luca, C. Umeton, and I. C. Khoo, Appl. Phys. Lett. **77**, 7 (2000).
[2] C. Conti, M. Peccianti, and G. Assanto, Phys. Rev. Lett. **91**, 073901 (2003).
[3] G. Assanto, M. Peccianti, and C. Conti, Opt. Photonics News **14**, 45 (2003).
[4] C. Conti, M. Peccianti, and G. Assanto, Phys. Rev. Lett. **92**, 113902 (2004).
[5] C. Conti, G. Ruocco, and S. Trillo, Phys. Rev. Lett. **95**, 183902 (2005).
[6] M. Matuszewski, W. Krolikowski, and Y. Kivshar, J. Opt. Soc. Am. B. (to be published).
[7] Yu. S. Kivshar and G. P. Agrawal, *Optical Solitons: From Fibers to Photonic Crystals* (Academic Press, San Diego, 2003).
[8] E. A. Kuznetsov and A. M. Rubenchik, Phys. Rep. **142**(3), 103 (1986).
[9] M. Peccianti, K. A. Brzdiakiewicz, and G. Assanto, Opt. Lett. **27**, 1460 (2002).
[10] G. Assanto and M. Peccianti, IEEE J. Quantum Electron. **39**, 13 (2003).
[11] M. Peccianti, C. Conti, G. Assanto, A. de Luca, and C. Umeton, Nature (London) **432**, 733 (2004).
[12] A. Fratalocchi, M. Peccianti, C. Conti, and G. Assanto, Mol. Cryst. Liq. Cryst. **421**, 197 (2004).
[13] A. Alberucci, M. Peccianti, G. Assanto, A. Dyadyusha, and M. Kaczmarek, Phys. Rev. Lett. **97**, 153903 (2006).
[14] A. Fratalocchi, A. Piccardi, M. Peccianti, and G. Assanto, Opt. Lett. **32**, 1447 (2007).
[15] A. Fratalocchi, A. Piccardi, M. Peccianti, and G. Assanto, Phys. Rev. A **75**, 063835 (2007).
[16] C. García-Reimbert, A. A. Minzoni, T. R. Marchant, N. F. Smyth, and A. L. Worthy, Physica D **237**, 1088 (2008).
[17] A. A. Minzoni, N. F. Smyth, and A. L. Worthy, J. Opt. Soc. Am. B **24**, 1549 (2007).
[18] B. D. Skuse and N. F. Smyth, Phys. Rev. A **77**, 013817 (2008).
[19] C. García–Reimbert, A. A. Minzoni, and N. F. Smyth, J. Opt. Soc. Am. B **23**, 294 (2006).
[20] C. García-Reimbert, A. A. Minzoni, N. F. Smyth, and A. L. Worthy, J. Opt. Soc. Am. B **23**, 2551 (2006).
[21] W. L. Kath and N. F. Smyth, Phys. Rev. E **51**, 1484 (1995).
[22] M. Abramowitz and I. A. Stegun, *Handbook of Mathematical Functions with Formulas, Graphs and Mathematical Tables* (Dover Publications, Inc., New York, 1972).